Geotextiles and Geomembranes 45 (2017) 320–330

Contents lists available at ScienceDirect

Geotextiles and Geomembranes

journal homepage: www.elsevier.com/locate/geotexmem

Investigation of soil-geosynthetic-structure interaction associated with induced trench installation

M.A. Meguid Associate Professor [a, *], M.G. Hussein Graduate Student [a], M.R. Ahmed Graduate Student [a], Z. Omeman Research Associate [a], J. Whalen Manager [b]

[a] Civil Engineering and Applied Mechanics, McGill University, Montreal, Quebec, H3A 0C3, Canada
[b] Plasti-Fab Ltd., Canada

ARTICLE INFO

Article history:
Received 26 June 2016
Received in revised form
4 April 2017
Accepted 7 April 2017
Available online 15 April 2017

Keywords:
Geosynthetics
Soil-structure interaction
EPS geofoam
Buried structures
Soil arching

ABSTRACT

The design of subsurface structures associated with transportation and other underground facilities, such as buried pipes and culverts, requires an understanding of soil-structure interaction. Earth loads on these structures are known to be dependent on the installation conditions. To reduce earth pressures acting on buried structures installed under high embankments, the induced trench method has been recommended and applied in practice for several decades. It involves the installation of a compressible material (e.g. EPS geofoam blocks) immediately above the buried structure to mobilize shear strength in the backfill material. A first step towards understanding this complex soil-geosynthetic-structure interaction and accurately modeling the load transfer mechanism is choosing a suitable material model for the geofoam that is capable of simulating compressive testing results. In this study, an experimental investigation is conducted to measure the changes in contact pressure on the walls of a rigid structure buried in granular backfill with an overlying geofoam layer. Validated using the experimental results, finite element analysis is then performed and used to study the role of geofoam density, thickness and location on the load transferred to the buried structure. Conclusions are made regarding the effect of modeling EPS inclusion as a non-linear material and the role of EPS configuration on the earth pressure distribution around the buried structure.

1. Introduction

The installation of a buried structure in soft ground is known to cause a redistribution of the in-situ stresses. The relative stiffness of the structure to the surrounding soil has a significant impact on the magnitude and distribution of vertical pressures on the walls of the structure. For a rigid conduit installed using the embankment construction method, the vertical earth pressure is generally greater than the weight of the soil above the structure because of negative arching. Induced trench installation (also called the imperfect ditch or ITI method) has been often used to reduce the vertical earth pressure on rigid conduits. The method involves installing a compressible layer immediately above the conduit to generate positive arching in the overlying soil. The presence of this compressible layer reduces the stiffness of the soil column to be less than that of the surrounding soil. The Canadian highway bridge design code (CSA, 2006) and the AASHTO LRFD bridge design specifications (AASHTO, 2007) provide guidelines for estimating earth loads on positive projecting culverts, but not for culverts installed using the induced trench technique. This construction method has been an option used by designers to reduce earth pressures on rigid conduits buried under high embankments. However, recent doubts related to the induced trench method has left many designers uncertain as to the viability of this construction technique (McAffee and Valsangkar, 2008).

The significant effects of the relative soil movement above and adjacent to buried conduits on the earth pressure distribution was noted in the early 1900s. It is believed that Brown (1967) was the first to quantify the pressure reduction effect of hay layers placed above a rigid culvert using the finite element method. Since then, several researchers studied the relevant soil-structure interaction using experimental testing and field instrumentation (e.g. Sladen and Oswell, 1988; Vaslestad et al., 1993; Liedberg, 1997; Sun et al., 2011; Oshati et al., 2012), as well as numerical modeling (Kim and Yoo, 2002; Kang et al., 2008; Sun et al., 2009; McGuigan and

* Corresponding author.
E-mail address: mohamed.meguid@mcgill.ca (M.A. Meguid).

http://dx.doi.org/10.1016/j.geotexmem.2017.04.004
0266-1144/

Valsangkar, 2010, 2011) to help understand the method and to address uncertainties with this design approach.

Induced trench method has also been used to protect structures against surface blast (e.g. De et al., 2016; Murillo et al., 2009; Wang et al., 2006) and to improve the seismic resiliency of pipelines and buried structures (e.g. Lingwall and Bartlett, 2014). In addition, the installation of EPS geofoam blocks against the sides of a buried structure has been used to further reduce earth pressures on culverts under high earth loads (e.g. Jiang and Gu, 2008). Although some field results have been reported, little research has been done to confirm the pressure re-distribution on the walls of the structure under these conditions.

To analyze problems involving EPS inclusion, the geofoam material is often approximated as a linear elastic-perfectly plastic (e.g. Takahara and Miura, 1998) or nonlinear elasto-plastic material (e.g. Hazarika, 2006). Other nonlinear models have been proposed to capture the material response under triaxial loading (e.g. Chun et al., 2004; Leo et al., 2008; Ekanayake et al., 2015). Index tests performed on EPS blocks of different densities show that the material exhibited a nonlinear behavior for compressive strains greater than 1%, associated with a reduction in Young's modulus beyond this strain Level (Ertugrul and Trandafir, 2011). This is particularly true for low density EPS material. To capture this behavior, a numerical model that is capable of simulating the material response and replicate the experimental data is, therefore, needed.

1.1. Scope and objective

This study utilizes both physical and numerical modeling to investigate the earth pressure distribution on a rigid box-shaped structure buried in granular material and overlain by EPS compressible inclusion. A laboratory investigation is first conducted to measure the contact pressure distribution on the walls of the buried box structure using the tactile sensing technology. A material model that is capable of capturing the nonlinear behavior of soft EPS geofoam is used to model compressive index tests performed on different EPS samples. A finite element analysis is carried out to simulate the laboratory experiments and calculate the earth pressure distributions on the walls of the buried structure. The effects of several parameters, including EPS density, thickness, and location are also evaluated. In addition, the changes in earth pressure distribution on the culvert due to the placement of EPS geofoam blocks against the sidewalls are also examined. The analyses presented throughout this study have been performed using the general finite element software ABAQUS/Standard, version 6.13 (ABAQUS, 2013).

2. Experimental setup

The experimental setup used in this study consists of an instrumented hollow structural steel section (HSS) embedded in a test chamber as shown in Fig. 1. The section dimensions are chosen to represent a 1.25 m span culvert scaled down one-fifth in size. The HSS is instrumented using tactile sensing pads wrapped around the middle third of the structure. The test chamber was designed to accommodate an air bag underneath a top plate that is bolted to the box using eight high-tensile steel rods 1-inch in diameter. The top plate has a flat surface supported by a grid of steel beams with high rigidity. The use of an air bag ensures uniform load distribution at the soil surface.

Typical EPS densities used in practice for these applications are 15 and 22 kg/m^3 and, therefore, they were adopted in the laboratory experiments. The thickness of the EPS block has been chosen such that it represents about 25% of the height of the box. This ratio has been shown by researchers (e.g. Vaslestad et al., 1993; McGuigan and Valsangkar, 2010) to be acceptable and allow for soil arching to develop with little effect on contact pressures.

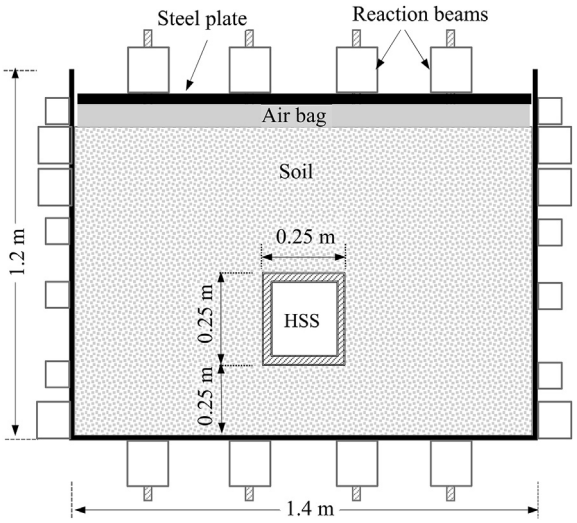

Fig. 1. A cross section showing the location of the buried structure.

2.1. Test chamber

The chamber dimensions (1.4 × 1.2 × 0.45 m) are selected such that they represent two-dimensional plane strain loading conditions. The rigid walls are placed far enough from the instrumented HSS section to minimize boundary effects. The distance from each side of the HSS to the sidewall is 0.575 m, which is more than twice the width of the buried structure (Bloomquist et al., 2009). All steel wall surfaces were painted with epoxy coating and a double layer of plexiglass (2 mm thick) was placed on the back and front of the strong box. The layer in contact with the box was fixed, while the layer in direct contact with the soil was free providing a smooth sliding surface and hence minimizing friction effects. Similar boundary treatment techniques have been successfully used by researchers in both reduced and full-scale experiments (e.g. Hong et al., 2016; Ahmed et al., 2015; Zamani et al., 2011).

Due to the high pressure induced by the air bag on the walls of the chamber, the surrounding area received extra reinforcement by placing four (two in the front and two in the back) 6-inch HSS steel sections around the zone where the airbag is located. The front and backsides of the container was monitored during the experiment using six dial gauge stations. No wall movement was recorded during the test, which confirms that the test chamber is sufficiently rigid for the purpose of these experiments.

Dry sandy gravel with D_{50} of 0.6 mm and average unit weight of 16.28 kN/m^3 was used as backfill material. Sieve analysis, conducted on selected samples, indicated a coarse-grained material with 77% gravel and 23% sand. The friction angle of the backfill soil is determined using direct shear tests performed on soil samples, of comparable density to that of the experiment, and is found to be 47°.

2.2. Buried HSS structure

A rigid HSS section with dimensions 0.25 × 0.25 × 0.435 m and 1 cm in wall thickness is used as a buried structure throughout this study. The structure is instrumented using three custom-made pressure sensing pads (TactArray sensors) placed directly on the upper (S1), side (S2) and lower (S4) walls as shown in Fig. 2. Each pad contains two sets of orthogonal electrodes (plates) separated

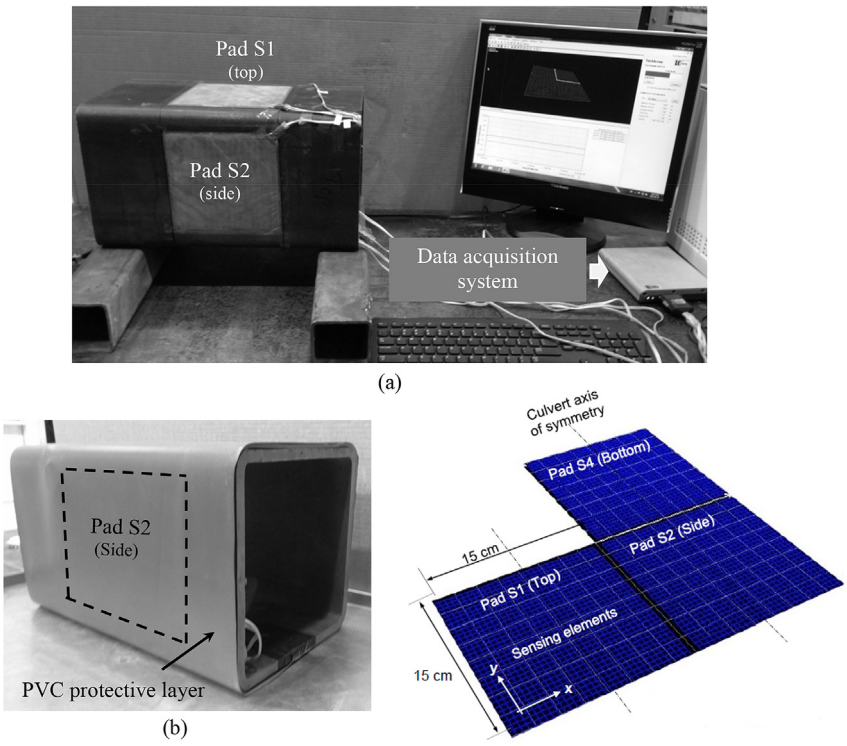

Fig. 2. Instrumentation of the buried structure: (a) installation of sensing pads (b) placement of the protective layer.

using a flexible insulator that acts as a spring allowing for conformable and stretchable pad designs. When a load is applied on the capacitive sensors, it changes the distance between the plates resulting in a change in capacitance (Dahiya and Valle, 2013). The changes in capacitance is converted into a change in voltage by using an appropriate circuit and a measure of applied force is then obtained. The recorded earth pressure using the TactArray sensing pads ranges from 0 to 140 kPa for the upper and side walls and from 0 to 350 kPa for the lower wall. Each sensing pad contains 255 square-shaped sensors that are protected from the backfill abrasion by wrapping the whole conduit with a thin layer of PVC as shown in Fig. 2. The pads are also laminated at the manufacturing stage using smooth plastic sheets to alleviate the shearing effects. The displacement of the HSS section was monitored during the tests and was found to experience insignificant movement in the vertical direction due to the compression of the bedding layer. As the box is relatively rigid compared to the backfill material, no deformation was recorded within the section under the maximum applied pressure.

It is worth noting that the ratio between the minimum dimension of the structure (B = 250 mm) and the average grain size of the backfill (0.6 mm) is about 416 which is twice the ratio required to avoid potential scaling effects (Randolph and House, 2001). In addition, the backfill height was chosen to be twice the width of the structure. Although the height of the soil cover is less than that needed to reach the plane of equal settlement, the measured pressures are considered acceptable for the validation of the numerical model. Further analysis are performed using larger soil cover to minimize the boundary effects and ensure uniform pressure distribution above the structure.

2.3. Calibration of the pressure sensors

Calibration of the sensors was initially performed by the manufacturer utilizing a chamber equipped with a thin air bladder that applies a uniform pressure to the sensing pads. In addition, prior to use, sensors were preconditioned and calibrated according to the manufacturer's recommendations using repeated load cycles. A pneumatic actuator was used to apply the vertical pressure directly over the sensing pad and the response was measured using the data acquisition system.

A series of tests was also conducted to study the effect of the protective layer on the measured pressure. The response was compared before and after the addition of the protective layer (Fig. 3). The results show that the sensing pads are capable of accurately capturing the applied pressure and the chosen protective material is stiff enough and does not cause any distortion of the pressure readings.

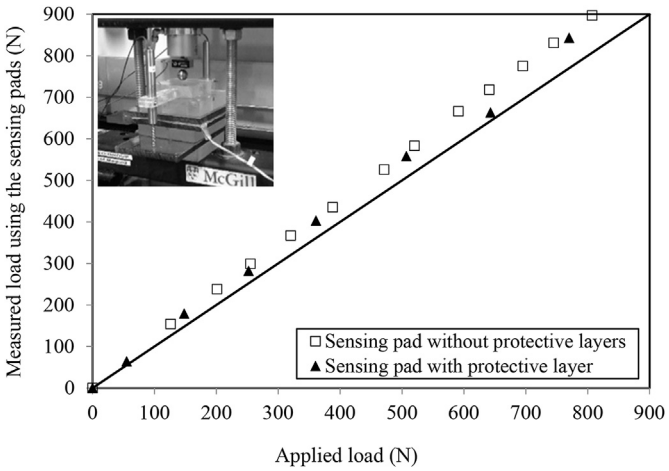

Fig. 3. Calibration of the pressure sensors.

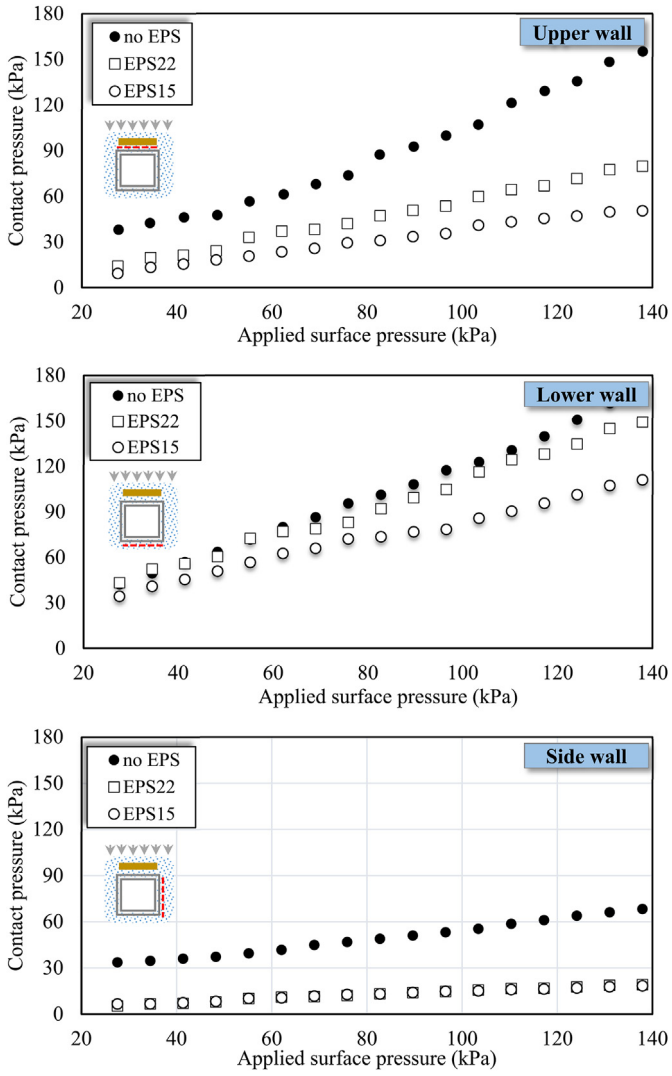

Fig. 4. Average earth pressures on the walls of the culvert.

3. Experimental procedure and results

A total of nine experiments were conducted including three benchmark tests with only the instrumented HSS box inside the backfill and then two sets of tests were performed for different geofoam densities. For all tests, a well-tamped bedding zone of 25 cm in height was created to ensure consistent initial conditions. The HSS box was placed over the bedding layer and leveled to minimize concentration of stresses under the box. Soil placement continued in layers over the HSS up to the desired height resulting in a backfill thickness of 0.5 m.

After the completion of each test, the chamber was emptied using a vacuum machine connected to a collection barrel. The HSS was then retrieved and the setup is prepared for the next test.

The average recorded earth pressures around the HSS structure overlain by a geofoam block are summarized in Fig. 4. The results for the benchmark tests with no geofoam (indicated by dark circles) are also provided for comparison purposes. The contact pressure generally increased with the increase in surface pressure. At an applied pressure of about 140 kPa, the average readings of the benchmark case at the upper, lower and sidewalls are 155, 169 and 68 kPa, respectively. The effects of placing two different expanded polystyrene (EPS) materials, namely EPS15 and EPS22 (properties are given in Table 1) above the buried structure are evaluated at the three investigated locations. Results showed that contact pressure decreased to 50 kPa and 111 kPa on the upper and lower walls, respectively. Changes measured on the sidewalls were found to be less significant for both types of EPS materials.

Downward drag forces represent the added contact pressure at the lower wall due to the development of shear stresses along the sidewalls of the structure. It is usually augmented when induced trench technique is used. The contribution of the drag forces to the contact pressures under the buried box was estimated by comparing the measured pressures on the upper wall (adding the weight of buried box ≈ 340 N or 3 kPa) with the contact pressure measured on the lower wall. The difference between the upper and lower wall readings for the benchmark case (no geofoam) was found to be 15 kPa, which corresponds to an increase in pressure of 12 kPa (about 9%) on the lower wall due to the downward drag forces. For the induced trench condition, the pressure change was found to be about 22 kPa that corresponds to an increase in

Table 1
Properties of the backfill, EPS and HSS structure used in the analysis.

Backfill soil properties					
Density (kg/m^3)	E′ (MPa)	ν′ Poisson's ratio	ϕ′° Friction angle	ψ° Dilation angle	c′ Cohesion (MPa)
1628	150	0.3	47	15	0
EPS geofoam properties					
EPS material type			Density (kg/m^3)	E (MPa)	(ν) Poisson's ratio
EPS39			38.4	17.8	0.15
EPS22			21.6	6.91	0.10
EPS15			14.4	4.20	0.10
Box material properties					
Hollow square section (HSS 250) 250 × 250 × 10 mm			Density (kg/m^3) 7850	E (GPa) 200	(ν) Poisson's ratio 0.3
Interface parameters					
Interface type			Friction coefficient (μ)		E_{slip}
Soil-EPS			0.60		0.005
Soil-PVC			0.45		
EPS-PVC			0.30		

pressure of about 30% for both EPS15 and EPS22.

3.1. Comparison with analytical solution

Fig. 5 shows a summary of the measured and calculated pressures normalized with respect to the positive projecting case (embankment technique). The figure demonstrates that the positive projecting method, with no compressible inclusion, results in a contact pressure that is 25% more than the overburden pressure of the soil at a given embankment height. This is attributed to the fact that the buried structure is stiffer than the surrounding soil resulting in negative arching. Marston induced trench method (Marston, 1930) predicted a pressure ratio of about 0.4 or 40% of the earth load on the upper wall if a compressible material was used (induced trench installation). The experimental results showed a pressure reduction that ranged from 0.38 for EPS22 to 0.35 for EPS15 as compared with the positive projecting method. This figure confirms that the measured earth pressures on the buried structure are consistent with the existing analytical solution. Details of the analytical study can be found elsewhere (Ahmed, 2016).

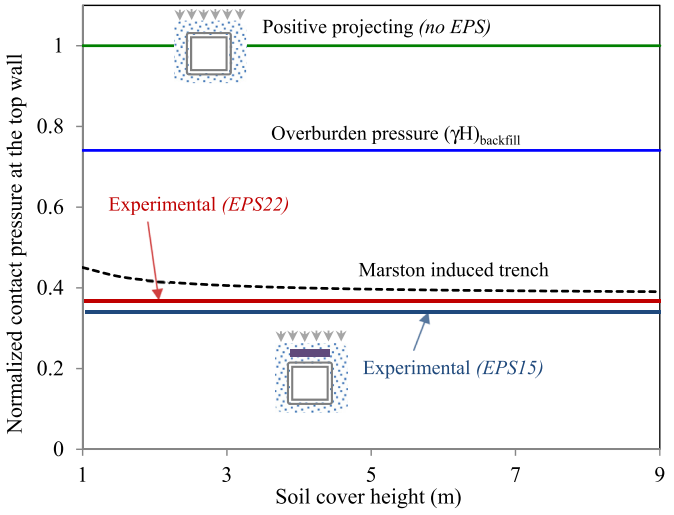

Fig. 5. Comparison of measured contact pressures with analytical solution.

4. Numerical analysis

Modeling soil-geofoam-structure interaction requires careful selection of material models that are suitable for each of the system components. While the buried structure and the backfill material can be represented using existing material models in most commercial software packages, modeling the compressible EPS material was found to be challenging, particularly at high strain levels.

Index test results obtained from a series of uniaxial unconfined compression tests on 125 mm cubes of three different densities revealed that the geofoam generally behaves as a nonlinear elasto-plastic hardening material as shown in Fig. 6. To model the uniaxial tests up to 15% strain, a constitutive model that is capable of describing the details of material behavior is needed. The approach

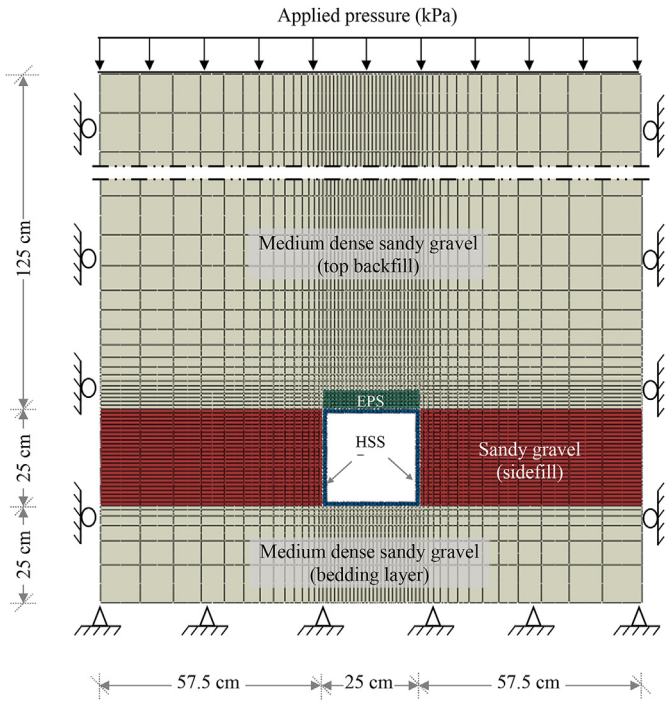

Fig. 7. The finite element mesh used in the parametric study.

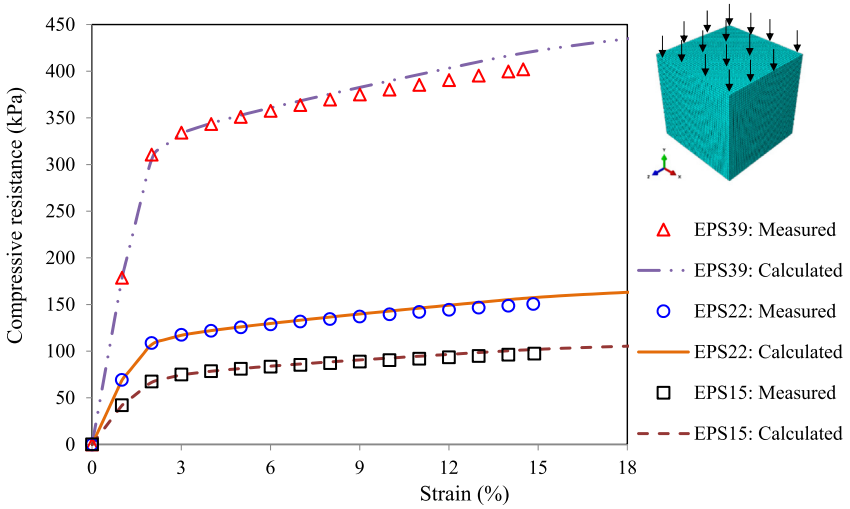

Fig. 6. EPS model performance: experimental versus calculated results.
(EPS properties are given in Table 1).

used to capture the different model features is described by Meguid and Hussein (2017).

Three-dimensional FE analyses are conducted to simulate the index tests for three EPS geofoam materials, namely, EPS15, EPS22, and EPS39. The cube geometry is discretized using 8-node linear brick elements (C3D8) with eight integration points. To simulate the uniaxial compressive test, the model is restrained in the vertical direction along the base and a compressive load is applied at the top using a prescribed velocity. Several mesh sizes were tested to determine a suitable mesh that brings a balance between accuracy and computing cost. An average element size of 3 mm was found to satisfy this balance and to produce accurate results. To validate the numerical model, the calculated and measured load-strain relationships are compared in Fig. 6. In general, the elasto-plastic constitutive model was found to reasonably represent the response of the material in both the elastic and plastic regions. This material model has been adopted for the EPS inclusion used in simulating the induced trench experiment.

4.1. Modeling soil-EPS-structure interaction

A series of 2D finite element analyses is performed using ABAQUS software to investigate the role of geofoam density, thickness, width and location on the changes in earth pressure on the buried structure and to confirm the experimental results with respect to the optimum EPS characteristics and location above the structure. The backfill soil is modeled using elasto-plastic Mohr-Coulomb failure criteria with non-associated flow rule. The HSS is treated as linear elastic material with density of 7850 kg/m^3. The Poisson's ratio and Young's modulus of the HSS are 0.3 and 200 GPa, respectively, which represent typical values for the HSS section No. 250 used in this investigation. The properties of the different materials used in the analysis are summarized in Table 1.

The finite element (FE) mesh that represents the geometry of the experiment, the boundary conditions, and the different soil zones around the HSS section is shown in Fig. 7. The mesh size was adjusted around the structure to provide sufficient resolution and accuracy within the studied area. Mesh sensitivity analysis was

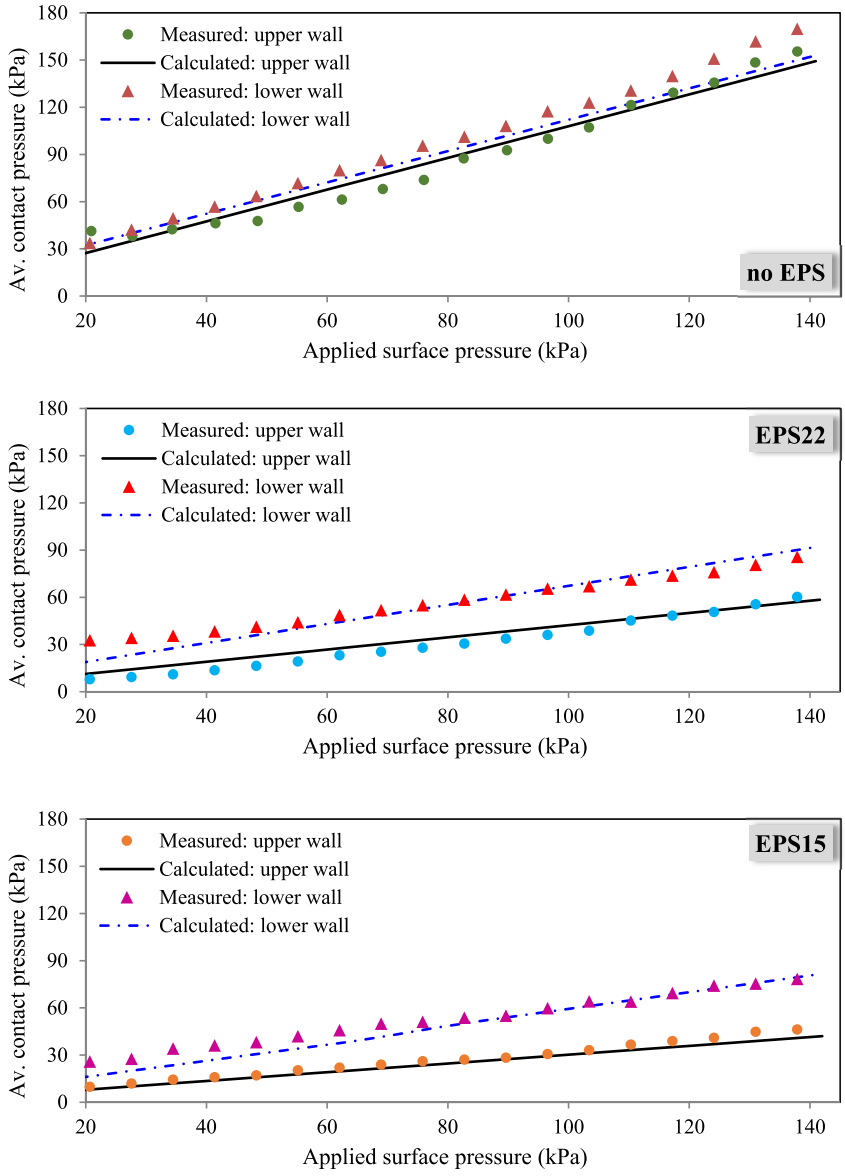

Fig. 8. Model validation for the cases of a) No EPS, b) EPS22 and c) EPS15.

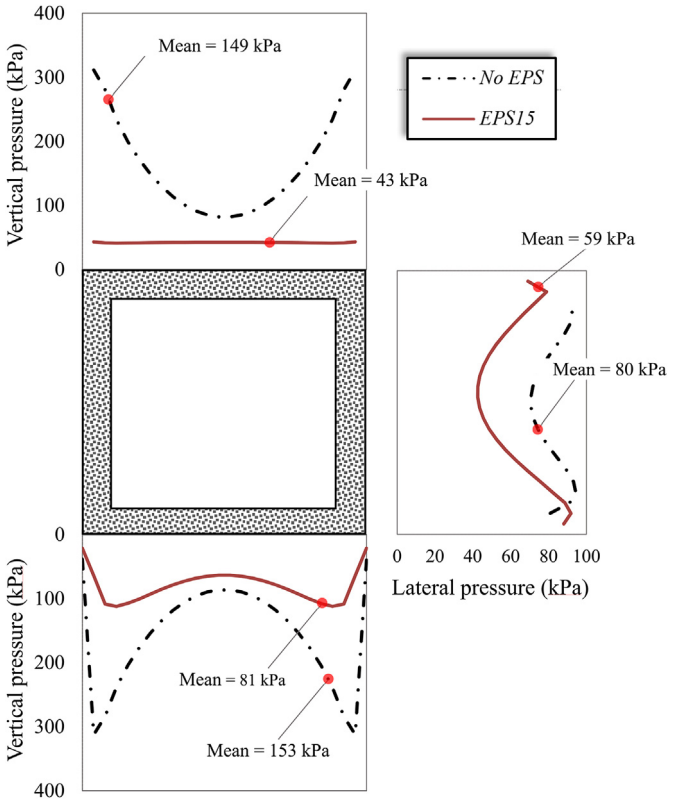

Fig. 9. Contact pressure distribution on the structure for surface pressure of 140 kPa.

performed by gradually reducing the element size from 50 mm to 10 mm while monitoring the soil response near the structure. A mesh with element size of 10 mm around the structure that increases to 100 mm at the boundary was found to strike the balance between the cost of the analysis and the accuracy of the calculated results. The used mesh comprises a total of 1962 quadratic plane strain elements (CPE8) and 6449 nodes. Boundary conditions were defined such that nodes along the vertical boundaries may translate freely in the vertical direction but are fixed against displacements normal to the boundaries (smooth rigid). The nodes at the base are fixed against displacements in both directions (rough rigid).

Three different contact conditions are considered in this study; namely, i) Soil-EPS interaction, ii) Soil-Structure interaction and iii) EPS-Structure interaction. These interactions are simulated using the surface-to-surface, master/slave contact technique available in ABAQUS. Contact formulation in 2D space covers both tangential and normal directions. In the tangential direction, Coulomb friction model with penalty algorithm is used to describe the shear interaction between the geofoam, the structure, and the surrounding soil. This model involves two material parameters- a friction coefficient (μ), and a tolerance parameter (E_{slip}). The shearing resistance (τ) is considered as a function of the shear displacement that represents the relative movement between the two contacted parties. On the other hand, a 'hard' contact model is used to simulate the contact pressure in the normal direction.

The interface friction angle between sand and EPS has been reported by several researchers (e.g. Horvath, 1995; Bartlett et al., 2000; Jutkofsky et al., 2000; Xenaki and Athanasopoulos, 2001; Stark et al., 2004; AbdelSalam and Azzam, 2016) and was found to range from 27° to 33° for different backfill materials. This range corresponds to a friction coefficient of 0.5–0.65. Given the internal friction angle for the backfill material used in this study ($\phi = 47°$) and the reported range of interface friction coefficient values, a soil-EPS interface friction coefficient of 0.6 is used in the analysis. The friction coefficient between the soil and the PVC sheet covering the buried structure is taken as 0.45 based on the values reported by Vaid and Rinne (1995). A summary of the parameters used to describe these interface conditions is given in Table 1.

4.2. Model validation

The numerical results are first validated by comparing the calculated pressures with the measured values for the three cases a) the benchmark test with no geofoam, b) using EPS15, and c) using EPS22. As shown in Fig. 8, the numerical model was able to capture the pressure changes, at the top wall, with a reasonable accuracy for the benchmark test as well as for the induced trench cases. Contact pressure increased linearly with the applied surface pressure with smaller initial values for the cases where EPS was installed above the buried structure. In general, the introduction of EPS geofoam block above the structure resulted in significant decrease in pressure, particularly for the upper and lower walls of the structure. For example, for an applied surface pressure of 140 kPa, the earth pressure on the upper wall decreased by 60% (from 149 kPa for the benchmark case to 60 kPa) for the induced trench installation using EPS22 and the reduction in pressure reached about 70% (43 kPa) when the EPS15 inclusion was introduced. Similar behavior was found for the lower wall with pressure reductions of 40% (90 kPa) and 45% (80 kPa) for EPS22 and EPS15, respectively.

4.3. Contact pressure distribution

The contact pressure distributions on the walls of the buried structure are illustrated in Fig. 9 before and after the introduction of a geofoam block (EPS15) above the structure. The distribution was generally characterized by stress concentration at the corners and was more pronounced at the upper and lower walls. Adding the geofoam block immediately above the upper wall resulted in a more uniform pressure distribution at that location, with a significant drop in pressure from an average value of 149 kPa–43 kPa. This corresponded to a geofoam compression of 0.66 mm or about 1.3% strain. It is also noted that the average pressure on the upper wall represents 100% of the overburden pressure for the positive projecting analysis (no EPS) and about 28% of that value for the ITI method. Similarly, the average pressure on the lower wall decreased from 153 kPa for positive projecting to 81 kPa for the ITI method. For the sidewalls, the average pressure represented 53% and 39% of the overburden pressure for the positive projecting and ITI method, respectively.

Although the above results are overall consistent with those reported by McAffee and Valsangkar (2008) using a linear elastic geofoam model, direct comparison of the calculated pressures may not be feasible due to the difference in test conditions and geofoam densities. Based on this study, modeling EPS10 (used in the above reference) as linear elastic material may provide approximate estimates of contact pressures in the small strain range. However, at higher applied pressure, and as the compressive resistance of the material approaches yielding, the linear elastic model may not be capable of capturing the correct strains developing in the EPS block.

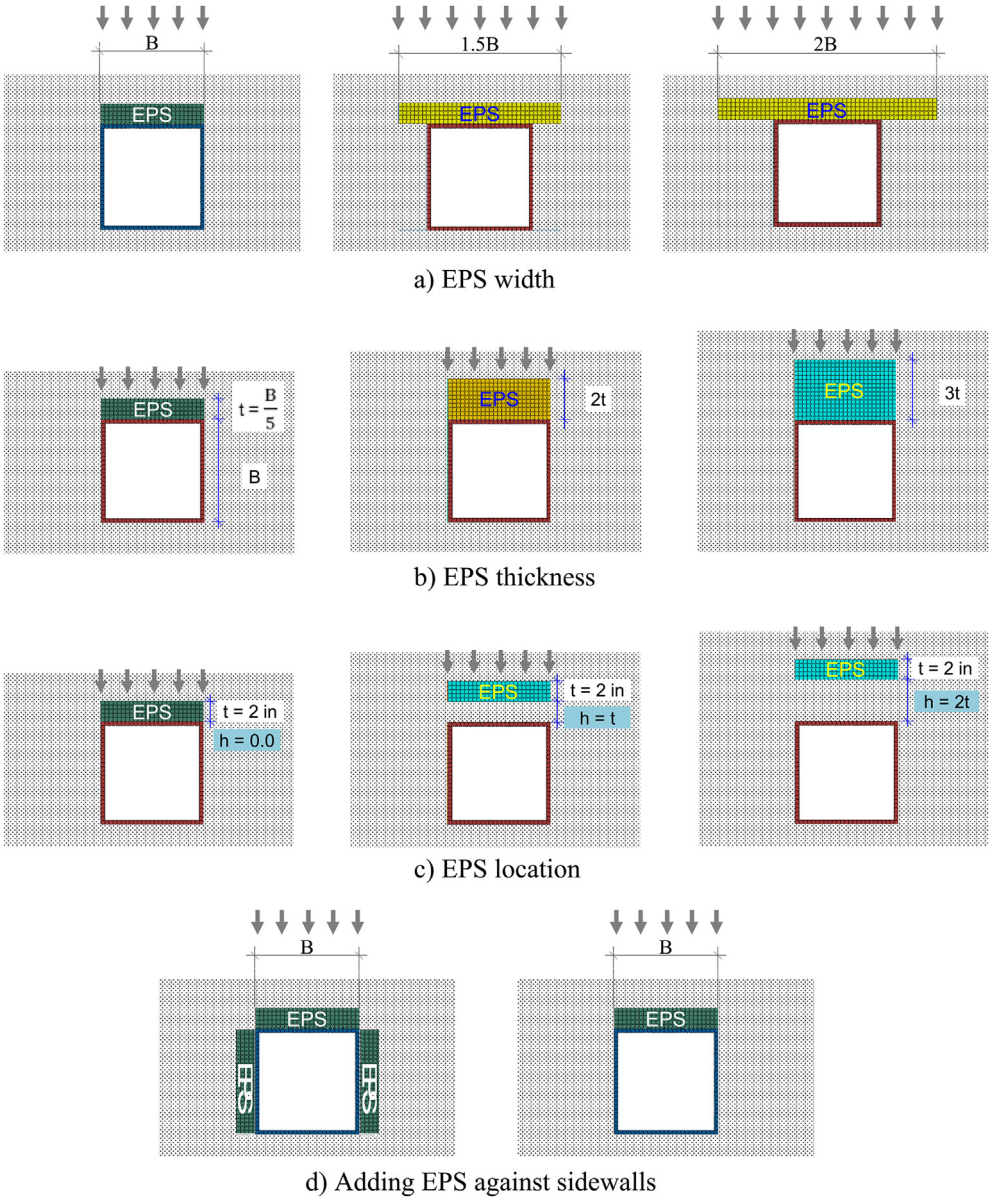

Fig. 10. A schematic of the investigated geometric parameters of the EPS block with respect to the buried structure.

4.4. Effect of EPS geometry

To study the effect of different parameters related to the EPS geometry and location with respect to the upper wall of the structure, three geometric parameters have been chosen, namely, EPS width, thickness and distance from the upper wall. Each of these parameters was incrementally increased in three steps and the changes in earth pressure are calculated and compared with the benchmark case (no EPS). A schematic showing the range of values used for each of the investigated parameters is shown in Fig. 10. It should be noted that EPS15 material is chosen for the analysis reported in this section.

4.4.1. Effect of EPS width

To evaluate the effect of the EPS block width on the contact pressure acting on the walls of the buried structure, the EPS thickness and density are kept constant at B/5 and 15 kg/m^3, respectively, while the width is incrementally increased from one to two times the width of the HSS section. The results are summarized in Fig. 11a, b and c for the upper, lower and sidewalls, respectively. It can be seen that increasing the width of the EPS from 1B to 2B led to 12% increase in contact pressure at the upper wall (Fig. 11a). For the lower and sidewalls, however, the contact pressure decreased by about 10%. This is considered to be insignificant given that twice the geofoam volume (from 1B to 2B) was used.

4.4.2. Effect of EPS thickness

The effect of the EPS thickness is examined in Fig. 12 for EPS15. The EPS width was chosen to be equal to that of the HSS section (width = 1B). The thickness is increased incrementally from 1/5B to 3/5B and the contact pressure is calculated for each case around the HSS box. At the upper wall (Fig. 12a), increasing the thickness of the EPS block to 3/5B resulted in pressure decrease of about 18%. No significant change was found for the lower and sidewalls with slight increase in contact pressure as shown in Fig. 12b and c.

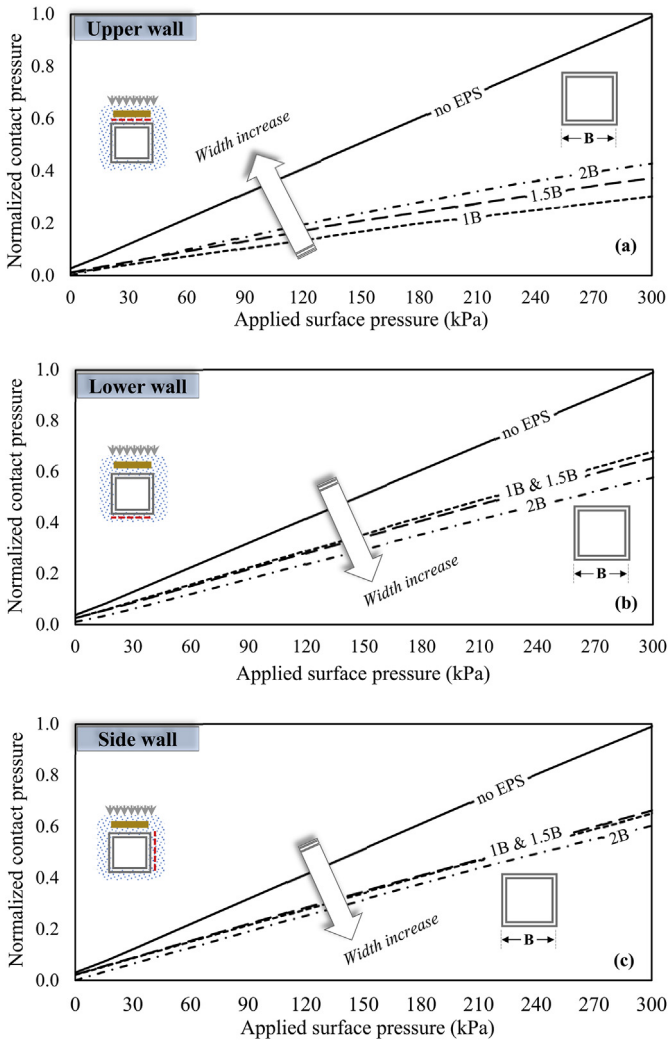

Fig. 11. Effect of EPS width on the change of earth pressure on the walls.

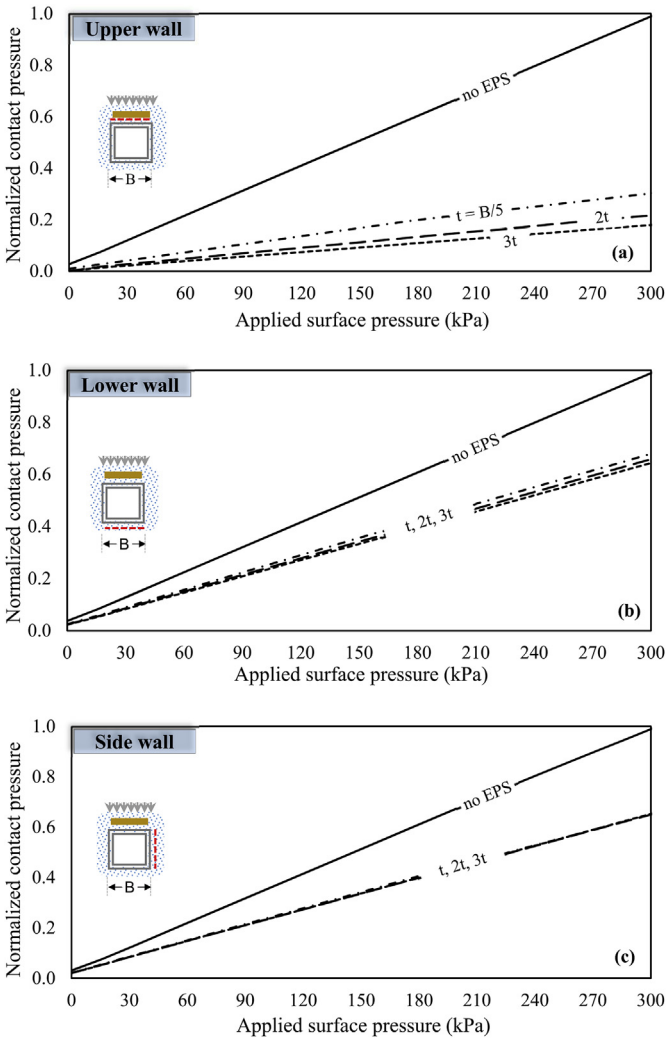

Fig. 12. Effect of EPS thickness on the change of earth pressure on the walls.

4.4.3. *Effect of EPS location*

Fig. 13 illustrates the effect of EPS block location with respect to the upper wall on the pressure transferred to the buried structure. The modeled geofoam block is EPS15 with 50 mm (2-inch) in thickness (t) placed at three different locations (h) above the structure such that h/t = 0, 1 and 2. It can be seen (Fig. 13a and b) that moving the EPS block by 100 mm (2t) led to a reduction in contact pressure at the upper and lower walls of about 10%. No significant change in pressure was found for the sidewalls (Fig. 13c) as a result of the change in EPS location.

4.5. *Effect of adding EPS blocks against the sidewalls*

To examine the effect of adding vertical geofoam blocks against the sidewalls (illustrated in Fig. 10d) on the contact pressure induced on the structure, a comparative analysis is performed using EPS15 and the results are summarized in Fig. 14. It can be seen that, for the investigated range of surface pressures, the addition of vertical EPS blocks had positive effects on the contact pressures as compared to the conventional ITI installation method. The largest effect was found at the sidewalls where pressures dropped from 60 kPa to 17 kPa, which corresponds to about 70% pressure reduction as shown in Fig. 14c. Despite the presence of the EPS15 block above the upper wall, the soil arching mechanism in this case resulted in a slight increase in pressure at the upper wall of the structure (Fig. 14a).

5. Summary and conclusions

In this study, the soil arching around a rigid HSS box buried in granular material was investigated using laboratory experiments and comprehensive numerical analysis. Expanded Polystyrene blocks are used as compressible material above the structure and the earth pressures on the upper, side, and lower walls are measured using tactile sensors and compared with positive projecting technique. Three benchmark experiments (without geofoam) and two sets of induced trench experiments using EPS15 and EPS22 were performed in this study. The height of the embankment was simulated by applying a uniform pressure on the surface of the soil using an airbag restrained by a strong reaction frame in both the vertical and lateral directions. The measured pressures at the upper wall are validated by comparing the average measured values with Marston's induced trench solution.

A numerical procedure for modeling the short-term response of EPS geofoam under uniaxial compression loading is developed using ABAQUS software. The model takes into account the different

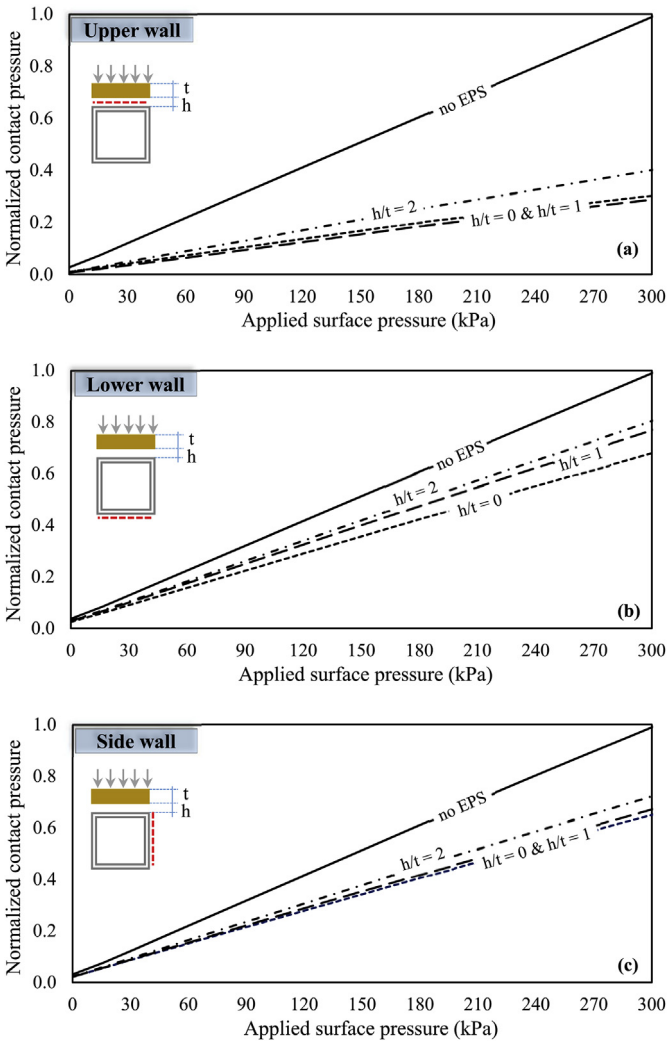

Fig. 13. Effect of EPS location on the change of earth pressure on the walls.

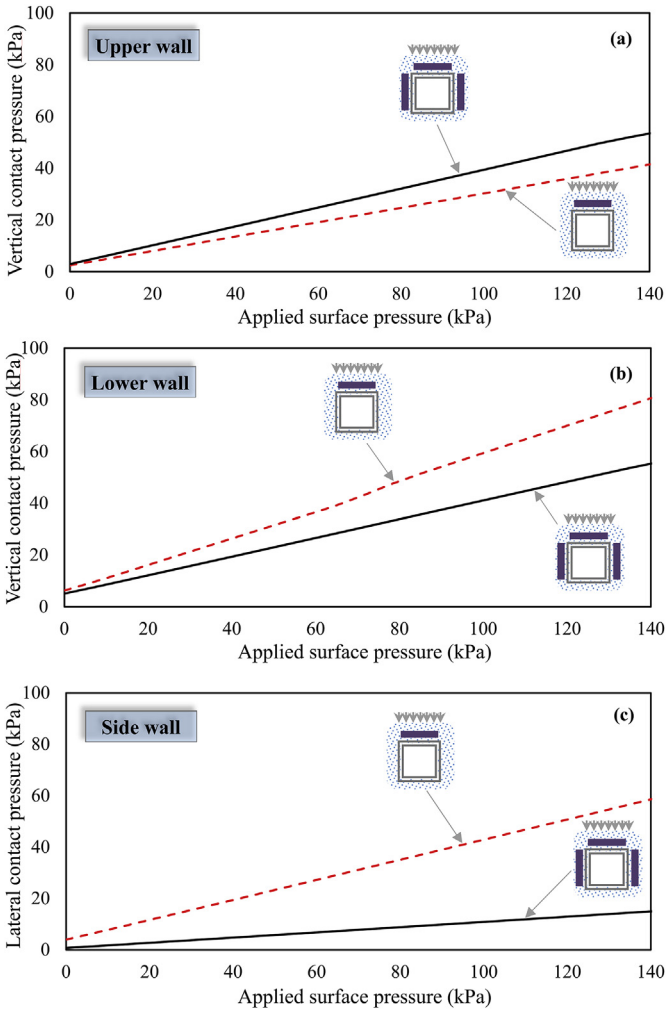

Fig. 14. Effect of EPS configuration on the change of earth pressure. (EPS15 geofoam).

features of the constitutive behavior responsible for the observed response. The material model is validated for three different EPS geofoam densities using index test results.

Contact pressure distribution on the walls of the buried box was found to be non-uniform with significant increase at the corners, particularly for positive projecting installation without geofoam. These stress concentrations decreased significantly after the addition of the EPS block above the structure.

A parametric study was performed to examine the role of EPS width, thickness and location on the earth pressures acting on the walls of the structure. For the investigated range of parameters, results showed that EPS density contributed significantly to the positive arching developed above the structure. Adding two EPS blocks against the sidewalls was found to significantly reduce the contact pressure acting on the side and lower walls; however, it led to a slight increase in pressure at the upper wall of the structure.

It should be noted that the above conclusions are based on a limited number of experiments conducted using a reduced scale model under 1g condition. Large-scale experiments may assist in verifying the above findings for large span culverts under full overburden pressure.

Acknowledgements

This research is supported by the Natural Sciences and Engineering Research Council of Canada (NSERC) CRD project No. 452760-13. The support of Plasti-Fab Ltd. throughout this study is appreciated.

References

AASHTO, 2007. American Association of State Highway and Transportation Officials, LRFD Bridge Design Specifications, fourth ed. Washington, D.C., USA.
ABAQUS, 2013. ABAQUS User's Manuals, Version 6.13. Dassault Systems Simulia Corp., Providence, RI, USA.
AbdelSalam, S.S., Azzam, S.A., 2016. Reduction of lateral pressures on retaining walls using geofoam inclusion. Geosynth. Int. 23 (6), 395–407.
Ahmed, M.R., 2016. Experimental Investigations into the Role of Geosynthetic Inclusions on the Earth Pressure Acting on Buried Structures. PhD. Thesis. Civil Engineering and Applied Mechanics, McGill University, Canada.
Ahmed, M., Tran, V., Meguid, M.A., 2015. On the role of geogrid reinforcement in reducing earth pressures on buried pipes. Soils Found. 5 (33), 588–599.
Bartlett, S., Negussey, D., Kimble, M., Sheeley, M., 2000. Use of geofoam as superlightweight fill for I-15 reconstruction. In: The 79th Annual Meeting for the Transportation Research Board. Transportation Research Board, Washington, DC, p. 21.
Bloomquist, D., Chen, Y., Crosby, M., 2009. Load Response Comparison between

Fiber and Steel Reinforced Concrete Pipe- Phase 2. Report developed for the Florida Department of Transportation, p. 187.
Brown, C.B., 1967. Forces on rigid culverts under high fills. J. Struct. Div. ASCE 93 (ST5), 195–215.
Chun, B.S., Lim, H.S., Sagong, M., Kim, K., 2004. Development of a hyperbolic constitutive model for expanded polystyrene (EPS) geofoam under triaxial compression test. Geotext. Geomembranes 22 (4), 223–237.
CSA, 2006. Canadian Highway Bridge Design Code - CHBDC. Canadian Standards Association, Mississauga, Canada, p. 930.
Dahiya, R.S., Valle, M., 2013. Robotics Tactile Sensing Technologies and System. Springer-Verlag, Berlin.
De, A., Morgante, A.N., Zimmie, T.F., 2016. Numerical and physical modeling of geofoam barriers as protection against effects of surface blast on underground tunnels. Geotext. Geomembranes 44 (1), 1–12.
Ekanayake, S.D., Liyanapathirana, D.S., Leo, C.J., 2015. Numerical simulation of EPS geofoam behaviour in triaxial tests. Eng. Comput. 32 (5), 1372–1390.
Ertugrul, O.L., Trandafir, A.C., 2011. Reduction of lateral earth forces acting on rigid nonyielding retaining walls by EPS geofoam inclusions. J. Mat. Civ. Engg. 23 (12), 1711–1718.
Hazarika, H., 2006. Stress-strain modeling of EPS geofoam for large-strain applications. Geotext. Geomembranes 24 (2), 79–90.
Hong, W.P., Hong, S., Kang, T.H.K., 2016. Lateral earth pressure on a pipe buried in soft grounds undergoing lateral movement. J. Struct. Integr. Maintenance 1 (3), 124–130.
Horvath, J.S., 1995. Geofoam Geosynthetic. Horvath Engineering, New York, USA, p. 217.
Jiang, F., Gu, A., 2008. Breakage mitigation method for culverts under high embankments using Eps geofoam. In: Liu, H., Deng, A., Chu, J. (Eds.), Geotechnical Engineering for Disaster Mitigation and Rehabilitation. Springer, Berlin, Heidelberg.
Jutkofsky, W., Sung, J., Negussey, D., 2000. Stabilization of embankment slope with geofoam. Transp. Res. Rec. 1736, 94–102.
Kang, J., Parker, F., Kang, Y.J., Yoo, C.H., 2008. Effects of frictional forces acting on sidewalls of buried box culverts. Int. J. Numer. Anal. Methods Geomechanics 32 (3), 289–306.
Kim, K., Yoo, C.H., 2002. Design Loading for Deeply Buried Box Culverts. Highway Research Center. Report No. IR-02-03. Auburn University, Alabama, USA, p. 215.
Leo, C.J., Kumruzzaman, M., Wong, H., Yin, J.H., 2008. Behavior of EPS geofoam in true triaxial compression tests. Geotext. Geomembranes 26 (2), 175–180.
Liedberg, N.S.D., 1997. Load reduction on a rigid pipe: pilot study of a soft cushion installation. Transp. Res. Rec. 1594, 217–223.
Lingwall, B, and Bartlett, S., 2014. Full-Scale Testing of an EPS Geofoam Cover System to Protect Pipelines at Locations of Lateral Soil DisplacementLoad Reduction on a Rigid Pipe: Pilot Study of a Soft Cushion Installation. Pipeline 2014, Portland, Oregon, August, pp. 605–615.
Marston, A., 1930. The Theory of External Loads on Closed Conduits in the Light of the Latest Experiments, Iowa Engineering Experiment Station, Bulletin 96, Volume XXVIII, Emes, Iowa.
McAffee, R.P., Valsangkar, A.J., 2008. Field performance, centrifuge testing, and numerical modelling of an induced trench installation. Can. Geotechnical J. 45 (1), 85–101.
McGuigan, B.L., Valsangkar, A.J., 2010. Centrifuge testing and numerical analysis of box culverts installed in induced trenches. Can. Geotechnical J. 47 (2), 147–163.
McGuigan, B.L., Valsangkar, A.J., 2011. Earth pressures on twin positive projecting and induced trench box culverts under high embankments. Can. Geotechnical J. 48 (2), 173–185.
Meguid, M.A., Hussein, M.G., 2017. A numerical procedure for the assessment of contact pressures on buried structures overlain by EPS geofoam inclusion. Int. J. Geosynth. Ground Eng. 3 (2), 1–14.
Murillo, C., Thorel, L., Caicedo, B., 2009. Ground vibration isolation with geofoam barriers: centrifuge modeling. Geotext. Geomembr. 27, 423–434.
Oshati, O.S., Valsangkar, A.J., Schriver, A.B., 2012. Earth pressures exerted on an induced trench cast-in-place double-cell rectangular box culvert. Can. Geotechnical J. 49 (11), 1267–1284.
Randolph, M.F., House, A.R., 2001. The complementary roles of physical and computational modelling. Int. J. Phys. Model. Geotechnics 1 (1), 1–8.
Sladen, J.A., Oswell, J.M., 1988. The induced trench method—a critical review and case history. Can. Geotechnical J. 25 (3), 541–549.
Stark, T.D., Arellano, D., Horvath, J.S., Leshchinsky, D., 2004. Guideline and Recommended Standard for Geofoam Applications in Highway Embankments. National Cooperative Highway Research Program (NCHRP), Report No. 529. Transportation Research Board, Washington, D.C., USA, p. 71.
Sun, L., Hopkins, T.C., Beckham, T.L., 2009. Reduction of Stresses on Buried Rigid Highway Structures Using the Imperfect Ditch Method and Expanded Polysterene (Geofoam). Kentucky Transportaion Center, Report No. KTC-07-14-SPR-228-01-1F. University of Kentucky, Kentucky, USA, p. 49.
Sun, L., Hopkins, T., Beckham, T., 2011. Long-term monitoring of culvert load reduction using an imperfect ditch backfilled with geofoam. Transp. Res. Rec. 2212, 56–64.
Takahara, T., Miura, K., 1998. Mechanical characteristics of EPS block fill and its simulation by DEM and FEM. Soils Found. 38 (1), 97–110.
Vaid, Y.P., Rinne, N., 1995. Geomembrane coefficients of interface friction. Geosynth. Int. 2 (1), 309–325.
Vaslestad, J., Johansen, T.H., Holm, W., 1993. Load reduction on rigid culverts beneath high fills: long-term behavior. Transp. Res. Rec. 1415, 58–68.
Wang, Z.-L., Li, Y.-C., Wang, J.G., 2006. Numerical analysis of attenuation effect of EPS geofoam on stress-waves in civil defense engineering. Geotext. Geomembranes 24, 265–273.
Xenaki, V.C., Athanasopoulos, G.A., 2001. Experimental investigation of the interaction mechanism at the EPS geofoam-sand interface by direct shear testing. Geosynth. Int. 8 (6), 471–499.
Zamani, S., El-Emam, M.M., Bathurst, R.J., 2011. Comparison of numerical and analytical solutions for reinforced soil wall shaking table tests. Geomechanics Eng. 3 (4), 291–321.